International Journal of e-Collaboration
Volume 17 • Issue 3 • July-September 2021

Measure of Nonlinearity With Application to Bearings-Only Target Tracking

Kausar Jahan, Koneru Lakshmaiah Education Foundation (Deemed), India
https://orcid.org/0000-0003-2162-8676

Sanagapallea Koteswara Rao, Koneru Lakshmaiah Education Foundation (Deemed), India

ABSTRACT

Using the recently proposed measure of nonlinearity (MoN), the authors try to find the magnitude of nonlinearity for passive target tracking with bearings-only measurements in underwater environment. The method derived to measure the nonlinearity is completely based on the state covariance matrices of the filters. It is tried to find the allowable magnitude of nonlinearity in terms of MoN with which a filter can perform to estimate the target motion parameters with required accuracy. In this paper, MoN values for different filters are computed for different scenarios. Results obtained in the Monte Carlo simulation are presented.

KEYWORDS

Estimation Theory, Kalman Filtering, Measure of Non-Linearity, Nonlinear Systems, Target Tracking

1. INTRODUCTION

A nonlinear problem in any area is generally difficult to address than a linear problem, and the complication increases with an increase in system nonlinearity. Although it is usually not difficult to ascertain if a system is linear or nonlinear, simply knowing that the system is nonlinear is not enough. It is prudent to know how much nonlinear the system is, i.e., to measure the nonlinearity of a problem. Such quantitative information about the problem reveals the root of the difficulty inherent in dealing with the problem, especially when comparing different processes.

The calculation of the nonlinearity of the system is as follows. For simplicity, a nonlinear function is approximated based on an equivalent linear function, as shown in Figure 1. Let $g\left(x\right)$ be a nonlinear function bounded in a domain with limits $\left(x_l, y_l\right)$ and $\left(x_u, y_u\right)$, and a linear function $f\left(x\right)$. The nonlinearity in the function corresponding to the straight line is calculated as the difference of $g\left(x\right)$ from $f\left(x\right)$ and is $\mathrm{g}\left(x\right) - f\left(x\right)$. Simply calculating the difference may make a zero-average of the difference between them (Emancipator & Kroll, 1993). So, the difference is squared, averaged, square rooted (Root Mean Squared), and then minimal values of the difference are calculated. But this

DOI: 10.4018/IJeC.2021070103

Figure 1. Sample of quantitative measure of nonlinearity

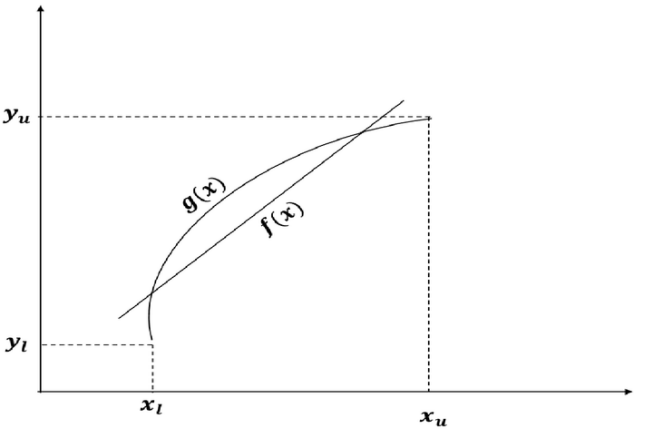

technique fails if the nonlinearity in the system is high enough. Hence an appropriate measure is needed to define nonlinearity levels in a system.

Considering the above-said method as a basis, for an overall system, the researchers developed various methods to measure nonlinearity. Nonlinear functions are generally linearised using Taylor series expansion. Beale's pioneering work (Beale, 1960) was the measurement of nonlinearity in terms of the deviation of nonlinear function from the linear function developed using Taylor series expansion. D. M. Bates et al. introduced a method to measure nonlinearity using relative curvatures (Bates & Watts, 1980), and J. Dunik et al. (2016) carried out a detailed survey on nonlinearity using D. M. Bates method. Li et al. (2019) constructed a combined nonlinear function using the time evolution and measurement functions in a filtering problem. M. Mallick et al., (2019) and X. R. Li et al., (2011) further continued the research on MoN. Their work represents a measure of the mean square distance between the given nonlinear system and a subset of all linear systems in a functional space.

Similar methods for measurement of nonlinearity are proposed in (Bucci et al., 2001; Li, 2012) for different applications. Usual methods for measuring nonlinearity can be broadly classified as follows. 1. A general measurement of nonlinearity function by its divergence from the linear function. 2. A specific measure of nonlinearity by using the bend in the nonlinear function at some reference point (Liu & Li, 2015).

The methods used to measure the nonlinearity are commonly known as Measure of Nonlinearity (MoN). Sultana et al. (2019) and X. R. Li et al. (2011) introduced an MoN calculation based on the state covariance matrix generated in the filtering algorithm. Work on these concepts continued and extended to bearings-only tracking (BOT) and ground moving targets using UKF and PF in (Sultana et al., 2019). The authors are motivated by the work presented in (Bates & Watts, 1980; Dunik et al., 2016; Li, 2012; Sultana et al., 2019) to apply MoN for BOT in passive mode for underwater target tracking using measurements from two different sensor arrays.

MoN of the system helps in determining the performance of the estimator, i.e., the extent of nonlinearity for which a filter can perform with acceptable error in estimated target parameters. In BOT, the nonlinearity of the process may change with change in the observer or target course or speed. This research calculates the nonlinearity in BOT with different target courses for different filtering algorithms. For the same scenario, MoN may differ with different filtering algorithms as MoN calculation is completely based on the state covariance matrices generated by the respective algorithms. Filter with a transformed or linearized measurement model may have lower MoN than a filter using the measurement model without any modification.

In an underwater scenario, BOT in passive mode is widely used. The signals radiated from the target are converted into bearing measurements to find the target path. These signals can be machinery noise from a target and are detected by an increase in energy above ambient at a certain bearing. Tracking a target using only bearing measurements is called BOT, and literature of BOT is available since 1979 (Aidala, 1979). In general, the 2D Cartesian state vector is used in finding the position and velocity of a target. Measurements are presumed to be available continuously for every second. Underwater observer contains, in general, single sonar, and hence observer carries out 'S' maneuver to make the process observable (Zhang et al., 2017; Zhu et al., 2012). The bearing measurements are nonlinearly related to the target state vector (Simon, 2006), and the 'S' maneuver is always not suitable. Proper change in bearing rate is enough for the process to be observable. So,the observer is recommended to follow certain maneuvers to achieve the bearing rate making the process observable (Koteswara Rao, 2005; Koteswara Rao, 2018).

To eliminate the divergence in solution and to improve the state estimation accuracy, several filtering algorithms are in use (Karthikeyan et al., 2019; Paul & Raja, 2017; Praveen Sundar et al., 2020; Umamaheswaran et al., 2019; Velliangiri et al., 2020; Vinoth Kumar et al., 2019; Vinoth Kumar et al., 2020). researchers developed several techniques with a difference in applicability and computational complexity (e.g., Extended Kalman Filter (EKF), Unscented Kalman Filter (UKF), and Particle Filter (PF) were developed. For example, in EKF, the nonlinearity in process is reduced by linearizing the system nonlinearities by using Taylor series expansions. It is a sub-optimal filter for the systems with low levels of nonlinearity. Other filters like UKF and PF use the deterministic resampling method for target state estimation. Hence, the MoN calculated differs for the same scenario with different filtering algorithms.

In this research paper, the authors would like to extend the MoN analysis for BOT with bearings-only measurements for various scenarios, using three different filterings (Koteswara Rao, 2005; Simon, 2006) algorithms, EKF, modified gain bearings-only extended Kalman filter (MGBEKF) and UKF. The maximum/minimum nonlinearity with which a filter can perform well and provide consistent results is analyzed for the BOT application. The MoN values at the samples where the solution is obtained are analyzed for several scenarios, and the same is explained in detail in Section 3 of the paper. The complexity in the computation of PF is higher than other filters, so it is not considered in this paper.The convergence analysis of the estimated motion parameters of the target is presented using root mean squared errors.

Mathematical modeling of state and measurement models for BOT and MoN are represented in Section 2. Section 3 is about the scenarios, acceptance criteria of the solution, simulation, and results obtained. Analyzation of MoN concerning different filtering (Koteswara Rao, 2005; Panigrahi & Bhuyan, 2017; Simon, 2006) algorithms for the BOT filtering process is also presented. Discussions on the results obtained and the inferences made from results are given in section 3. The paper is concluded in section 4. The sponsored project under which the research is being carried is acknowledged in section 5.

2. STATE AND MEASUREMENT MODELS

2.1. Bearings-Only Tracking

Consider the observer is at origin initially, and the target follows persistence speed and course. Target and observer movements are shown in Figure 2.

The observer state vector at time instant 'τ' (Aidala, 1979; Zhang et al., 2017) is given as:

$$S_o(\tau) = \begin{bmatrix} v_{xo}(\tau) & v_{yo}(\tau) & r_{xo}(\tau) & r_{yo}(\tau) \end{bmatrix}^T \quad (1)$$

Figure 2. Target and observer moments using bearings-only measurements

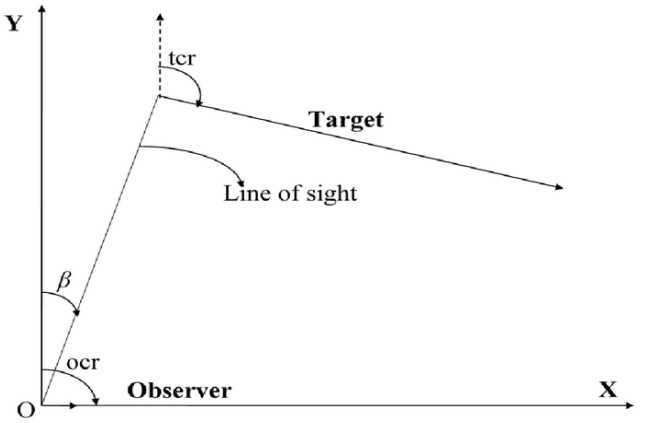

Here $v_{xo}(\tau)$, $v_{yo}(\tau)$, $r_{xo}(\tau)$, $r_{yo}(\tau)$ are the speeds and ranges of the observer in x and y coordinates respectively. The change in the observer position is obtained from its course and speed as:

$$dr_{xo}(\tau) = v_{xo}(\tau)\sin(ocr)t \tag{2}$$

$$dr_{yo}(\tau) = v_{yo}(\tau)\cos(ocr)t \tag{3}$$

Here $dr_{xo}(\tau), dr_{yo}(\tau)$ are the change in x and y coordinates of observer and ocr is the observer course and *t* is one second.

Similarly, the target state vector is given as:

$$S_t(\tau) = \left[v_{xt}(\tau) \quad v_{yt}(\tau) \quad r_{xt}(\tau) \quad r_{yt}(\tau)\right]^T \tag{4}$$

Here $v_{xt}(\tau)$, $v_{yt}(\tau)$, $r_{xt}(\tau)$, $r_{yt}(\tau)$ represent target's speed and range values in x and y coordinates respectively. Change in target position is obtained from its course and speed as:

$$dr_{xt}(\tau) = v_{xt}(\tau)\sin(tcr)t \tag{5}$$

$$dr_{yt}(\tau) = v_{yt}(\tau)\cos(tcr)t \tag{6}$$

Here $dr_{xt}(\tau), dr_{yt}(\tau)$ are the change in x and y coordinates of the target, and tcr is the course of the target, and *t* is the time of one second. The target's relative state vector (Jones et al., 2011; Simon, 2006; Zhu et al., 2012) is as follows:

$$S_s(\tau) = \left[v_x(\tau) \quad v_y(\tau) \quad r_x(\tau) \quad r_y(\tau)\right]^T \tag{7}$$

Here $v_x(\tau)$, $v_y(\tau)$, $r_x(\tau)$, $r_y(\tau)$ are relative values of speed and range in x and y coordinates respectively.

The relative state vector for the next time based on the present time state vector is given as:

$$S_s(\tau+1) = A(\tau)S_s(\tau) + b(\tau+1) + \omega C(\tau) \tag{8}$$

Here $A(\tau)$ is the system dynamics matrix given as:

$$A(\tau) = \begin{bmatrix} 1 & 0 & 0 & 0 \\ 0 & 1 & 0 & 0 \\ t & 0 & 1 & 0 \\ 0 & t & 0 & 1 \end{bmatrix} \tag{9}$$

$$b(\tau+1) = \begin{bmatrix} 0 \\ 0 \\ -\left(r_{xo}(\tau+1) - r_{xo}(\tau)\right) \\ -\left(r_{yo}(\tau+1) - r_{yo}(\tau)\right) \end{bmatrix} \tag{10}$$

and $C(\tau)$ is the process noise, and ω is given as:

$$\omega = \begin{bmatrix} t & 0 \\ 0 & t \\ t^2/2 & 0 \\ 0 & t^2/2 \end{bmatrix} \tag{11}$$

The covariance of the process noise is given as:

$$Q(\tau) = E\left[\left(\omega C(\tau)\right)\left(\omega C(\tau)\right)^T\right] \tag{12}$$

$$Q(\tau) = \sigma^2 \begin{bmatrix} t^2 & 0 & t^3/2 & 0 \\ 0 & t^2 & 0 & t^3/2 \\ t^3/2 & 0 & t^4/4 & 0 \\ 0 & t^3/2 & 0 & t^4/4 \end{bmatrix} \tag{13}$$

Here σ^2 is the variance of the process noise.

The measurement equation for this application has only bearing angles, and the bearing angle $\beta(\tau)$ is given as:

$$\beta\left(\tau\right) = \tan^{-1}\left(r_x\left(\tau\right) / r_y\left(\tau\right)\right) \tag{14}$$

The bearing measurement is always degraded with noise. So, the measured bearing is given as:

$$\beta_m\left(\tau\right) = \beta\left(\tau\right) + \eta\left(\tau\right) \tag{15}$$

Here $\eta\left(\tau\right)$ is the noise in the measurement. Here zero-mean additive process noise and measurement noise are considered. The system measurement equation is given as:

$$M\left(\tau\right) = h\left(\tau\right) S_s\left(\tau\right) + \gamma\left(\tau\right) \tag{16}$$

Here $h\left(\tau\right)$ matrix gives the relation between measurement and state of the system, and the measurement noise matrix is represented by $\gamma\left(\tau\right)$. For BOT using measurements from a single sensor array, $\gamma\left(\tau\right)$ is equal to $\eta\left(\tau\right)$ as $M\left(\tau\right)$ is a single measurement:

$$h\left(\tau\right) = \begin{bmatrix} 0 & 0 & \cos\beta\left(\tau\right) / R & -\sin\beta\left(\tau\right) / R \end{bmatrix} \tag{17}$$

$\gamma\left(\tau\right)$ is the measurement noise and is same as $\eta\left(\tau\right)$, and R is the range of the target from the observer, given as follows:

$$R = \sqrt{\left(r_x\left(\tau\right)\right)^2 + \left(r_y\left(\tau\right)\right)^2} \tag{18}$$

Measure of Nonlinearity

Mahendra Mallick et al. (2019) presented a new MoN for discrete-time nonlinear filtering problem that determines the deviation from linearity. They combined nonlinear function using the time evolution and measurement functions in a filtering problem. This MoN represents a measure of the mean square distance between the given nonlinear system and subspace of all linear systems in a functional space.

Equations (8) and (16) describe the discrete-time dynamic and measurement models for EKF, UKF, and MGBEKF (Koteswara Rao, 2005; Simon, 2006). The MoN is analyzed by considering the prediction and update cycle of the filtering algorithm during each time interval. For the BOT application, the functional space that contains all the linear and non-linear functions is taken as z(τ). The nonlinearity in BOT exists with the bearing measurement, which is tangentially related to the parameters taken in the target state vector. So, the state vector is a linear equation in four variables, and the measurement vector is a non-linear function in one variable. Hence the total functional space is taken as a combination of target state and measurement vectors.To analyze MoN, (8) and (16) are combined to form a single equation:

$$z\left(\tau+1\right) = \begin{bmatrix} S_S\left(\tau+1\right) \\ M\left(\tau+1\right) \end{bmatrix} = q\left(S_S\left(\tau+1\right)\right) + N\left(\tau+1\right) + B\left(\tau+1\right) \tag{19}$$

Here:

$$q\left(S_S\left(\tau+1\right)\right)=\begin{bmatrix}A\left(\tau\right)S_S\left(\tau\right)\\ h\left(\tau\right)S_S\left(\tau\right)\end{bmatrix} \tag{20}$$

$$N\left(\tau+1\right)=\begin{bmatrix}\omega C\left(\tau\right)\\ \gamma\left(\tau\right)\end{bmatrix} \tag{21}$$

$$B\left(\tau+1\right)=\begin{bmatrix}b\left(\tau\right)\\ 0\end{bmatrix} \tag{22}$$

Substituting (20), (21) and (22) in (19), $z\left(\tau+1\right)$ can be written as follows:

$$z\left(\tau+1\right)=\begin{bmatrix}A\left(\tau\right)S_S\left(\tau\right)\\ h\left(\tau\right)S_S\left(\tau\right)\end{bmatrix}+\begin{bmatrix}\omega C\left(\tau\right)\\ \gamma\left(\tau\right)\end{bmatrix}+\begin{bmatrix}b\left(\tau\right)\\ 0\end{bmatrix} \tag{23}$$

From (23), it can be said that $z\left(\tau\right)$ is linear in $N\left(\tau\right)$ and $B\left(\tau\right)$ but nonlinear in $S_S\left(\tau\right)$. The idea of measuring the deviation of the nonlinear function $S_S\left(\tau\right)$ from the best suited linear function is considered from (Sultana et al., 2019) as follows.

Let us consider a functional space F that gives a set of all linear and nonlinear functions of a random variable *x* with a specified distribution. Now divide the functional space into two sets such that one set contains all linear functions, $\mathcal{L}$ and other contains all nonlinear functions, $\mathcal{G}$. Assume a nonlinear function $q\left(\tau\right)$ that belongs to $\mathcal{G}$. The MoN is the deviation of $q\left(\tau\right)$ from linear functions set $\mathcal{L}$ and not from a single point in $\mathcal{L}$. This is done by calculating distances from $q\left(\tau\right)$ to every single point in $\mathcal{L}$ and evaluating the lower bound on the distances.

Consider J as the shortest distance between any two points, say $f1$ and $f2$, in F. J that suits the random nature of target parameters is given as follows:

$$J\left(f_1,f_2\right)=\left(E\left[\|\ f_1\left(x\right)-f_2\left(x\right)\|_2^2\right]\right)^{1/2} \tag{24}$$

Expression to find the closeness between $q\left(\tau\right)$ and $\mathcal{L}$ using (24) can be given as in (25):

$$J_\tau=\inf_{l\left(\tau\right)\epsilon\mathcal{L}}\left[J\left(l\left(\tau\right),q\left(\tau\right)\right)\right]=\inf_{l\left(\tau\right)\epsilon\mathcal{L}}\left(E\parallel l_\tau\left(x\right)-q_\tau\left(x\right)\|_2^2\right)^{1/2} \tag{25}$$

Let l be the set of all linear functions $l\left(x\right)=mx+n$ with dimension as that of q_τ. J_τ represents the un-normalized MoN. In the BOT application, till the process becomes observable, the error in the target state estimated parameters would be very high. As all the MoN values are calculated based on the target state covariance matrix, the MoN values will be too large, and hence they are normalized

to relate them with the MoN values at the time when the process becomes observable.The normalized version of J_τ is defined as follows:

$$V_\tau = J_\tau / \left[tr\left(P_{q(\tau)}\right)\right]^{1/2} \tag{26}$$

Here $P_{q(\tau)}$ is the covariance matrix of $q_\tau\left(x\right)$. Substituting for $l\left(x\right) = mx + n$ in equation (32) and differentiating with m and n, the un-normalized MoN is obtained as follows:

$$J = \left[tr\left(P_q - P_{qx}P_x^{-1}P_{qx}^{'}\right)\right]^{\frac{1}{2}} \tag{27}$$

Normalized MoN, J is given as:

$$V_\tau = \sqrt{\left(1 - tr\left(P_{qS}P_{\tau|\tau-1}^{-1}P_{qS}^{'}\right)\right) / tr\left(P_q\right)} \tag{28}$$

Here P_q is the covariance matrix of q, $P_{\tau|\tau-1}$ is the covariance of S_S, and P_{qS} is the covariance of q and S_S.

3. SIMULATION AND RESULTS

This research paper assesses MoN for three algorithms, EKF, UKF, and MGBEKF (Koteswara Rao, 2005; Simon, 2006), by implementing in MATLAB PC environment. The measurements are assumed to be available continuously for every second. The target is assumed to be having a different initial course in different scenarios, which are given in Table 1. Scenario with an initial bearing of 20o is like the scenario with an initial bearing of 0o turned by 20o. Hence the bearing value is all taken as 0o for simplicity. The MoN values change with change in course or speed or range of a target. In BOT underwater applications, the speeds of the submarines are generally maintained constantly

Table 1. Scenarios

Scenario number	Initial Range (m)	Initial Bearing (deg)	Target Speed (m/s)	Observer Speed (m/s)	Target Course (deg)
1	3000	0	12	8	100
2	3000	0	12	8	110
3	3000	0	12	8	135
4	3000	0	12	8	140
5	3000	0	12	8	145
6	3000	0	12	8	148
7	3000	0	12	8	155
8	3000	0	12	8	163
9	3000	0	12	8	170

and at lower speeds. If the speed is more or increasing, then the vehicle can be easily identified and tracked. So, a more generalized speed of target and observer are considered only with different target courses. The same process can also be analyzed with different target speeds.

The observer is maneuvering in its course based on the maneuver recommended for the observer in (Koteswara Rao, 2018). In the BOT application, only one type of measurement, i.e., bearing angles are available, and the parameters to be found are four (range in x and y coordinates, speed in x and y coordinates). So, to make the process observable, there must be a considerable change in bearing rate. In this process, the observer must make a maneuver that increases the bearing rate to a considerable amount so that the process becomes observable much faster.For BOT using maneuver recommendation, the observer first follows an initial line of sight direction for two minutes. Now, the side on which the target is present concerning observer is determined and the observer turns to move on the opposite side, i.e., if the target is on the right side of the observer, then the observer has to turn left side perpendicular to the line of sight for two minutes. The further maneuver of the observer is based on the angle on the target bow. If angle on target bow is less than 5°, then the same course of the observer is followed, if the angle on target bow is between 5° to 45° then the famous S- maneuver is followed, and if angle on target bow is greater than 45°, the observer follows L – maneuver. The noise in measurements is assumed to follow Gaussian distribution and is additive in nature.

The target state vector's initial estimate for the implementation of algorithms is taken as:

$$S_s\left(0/0\right)=\begin{bmatrix}5 & 5 & 5000\sin\beta_m & 5000\cos\beta_m\end{bmatrix}^T \tag{29}$$

The target velocities are each assumed as 5m/s. The target's initial position is calculated based on the Sonar Range of the Day (SRD), which is assumed to be 5000m.The initial state covariance matrix can be taken as a diagonal matrix if the uniform distribution of the initial state estimate is considered and is given as in eq. (30). The noise in measurements is assumed to have a standard deviation of 0.33 degrees:

$$P\left(0,0\right)=diagonal\begin{bmatrix}4v_x^2\left(0,0\right)/12\\4v_y^2\left(0,0\right)/12\\4r_x^2\left(0,0\right)/12\\4r_y^2\left(0,0\right)/12\end{bmatrix} \tag{30}$$

Monte-Carlo simulation (100 runs) is performed for the above-mentioned scenarios using MATLAB (Zhu et al., 2012) for all algorithms. The error in the estimated target parameters must be within the vicinity range of the weapon that has to be fired onto the target. The acceptance criteria are chosen based on the general torpedo homing zone values (as the application is an underwater scenario) and are evaluated in accordance with the true values calculated for the scenarios designed. The solution is said to be obtained only when the error in the estimated target parameters is less than the given values in acceptance criteria. Once the solution is obtained, the estimated target parameters can be used to release torpedo onto the target.

The performance is assessed based on the Root-Mean-Squared (RMS) error of the target parameters, and the solution is obtained based on the criteria of acceptance for 100 Monte-Carlo runs explained below.

Let the criterion to accept the solution is:

Error in range estimate <=2.66% of the true range

Error in course estimate <=1°
Error in speed estimate <=0.33m/s

Table 2 gives the convergence timings in seconds for different algorithms. Different parameters in analyzing the target motion are estimated with an acceptable error at different times. The overall time to estimate all parameters is the total convergence time. The target and observer movements for scenario 9 using maneuver recommendation with the EKF algorithm is shown in Figure 3. It can be seen from Figure 3 that the observer follows maneuver recommendation and the estimated target path is nearer to the simulated true target path, i.e., the solution is converged faster.

Table 2. Total convergence timings of algorithms in seconds

Filter	Scenario Number	Target Parameter			
		Range	Course	Speed	Total Convergence Time
EKF	1	NC	NC	NC	NC
	2	NC	NC	NC	NC
	3	NC	NC	NC	NC
	4	NC	684	NC	NC
	5	NC	NC	NC	NC
	6	NC	NC	NC	NC
	7	587	568	421	587
	8	202	163	244	244
	9	212	149	254	254
MGBEKF	1	259	270	279	279
	2	257	265	281	281
	3	216	204	249	249
	4	207	195	244	244
	5	201	188	232	232
	6	197	185	226	226
	7	190	169	216	216
	8	184	156	203	203
	9	172	144	194	194
UKF	1	NC	738	NC	NC
	2	253	252	278	278
	3	216	199	249	249
	4	212	190	246	246
	5	203	186	238	238
	6	200	183	231	231
	7	192	169	217	217
	8	188	157	211	211
	9	198	146	223	223

NC: No Convergence

Figure 3. Target and observer moments using EKF for scenario 9

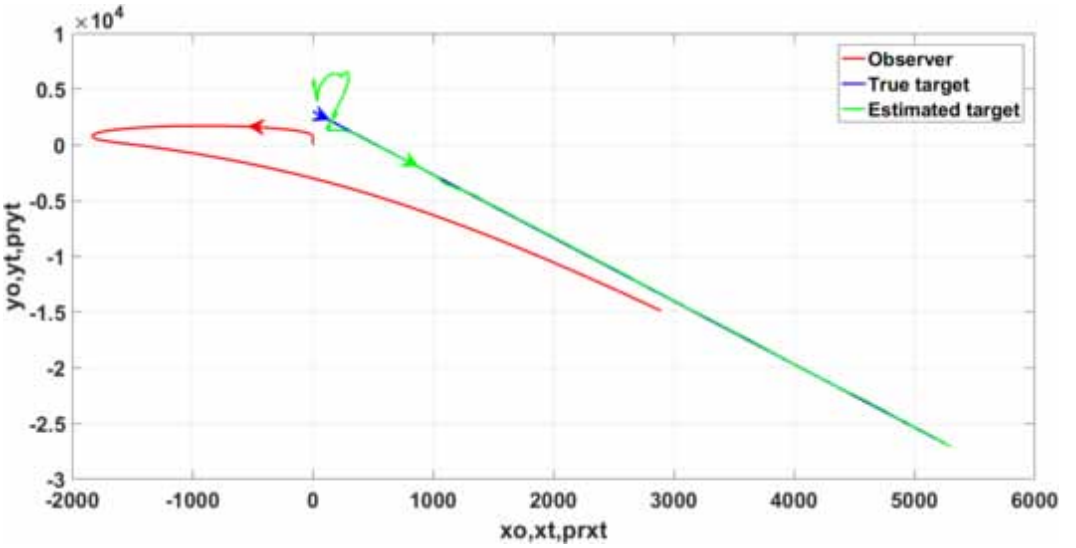

3.1. MoN of EKF

It is a known fact that EKF is unstable and a suboptimal nonlinear filter. The MoN for different scenarios using bearing measurements is calculated, and the following observations are made. MoN values for most of the scenarios start from low values and gradually increases to a maximum value, which then decreases gradually as shown in Figure 4. The solution is obtained when the MoN decreases after reaching its maximum MoN value. It can be observed from Table 3 data that the solution is obtained for the scenarios with maximum MoN values greater than 23. For scenarios 1 to 6, the MoN values are less than 23 and the solution is not obtained.

Table 3 gives the MoN values at convergence times of target parameters. The nonlinearity in the process is increasing with an increase in the target course angle. For all the target parameters, MoN values are increasing with an increase in the target course.

Figure 4. MoN values of EKF

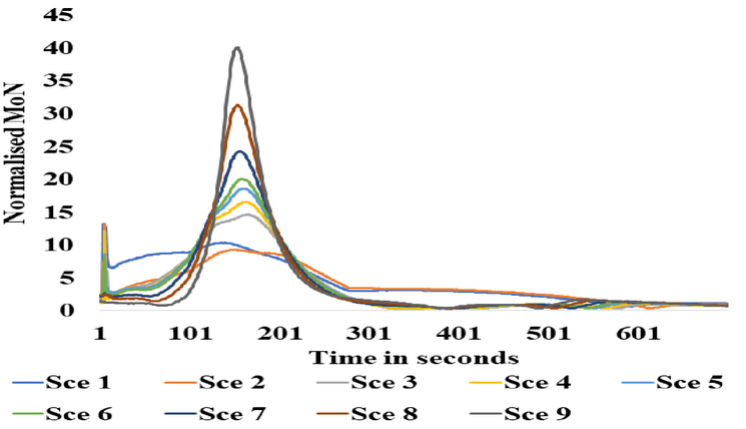

Table 3. Normalized MoN values of EKF at different time samples

Scenario number	RCT	MoN	CCT	MoN	SCT	MoN	Time	Maximum MoN
1	NC	-	NC	-	NC	-	5	13.22
2	NC	-	NC	-	NC	-	7	13.22
3	NC	-	NC	-	NC	-	166	14.67
4	NC	-	684	0.79	NC	-	166	16.54
5	NC	-	NC	-	NC	-	162	18.63
6	NC	-	NC	-	NC	-	160	20.07
7	587	1.36	568	1.43	421	0.67	157	24.31
8	202	7.35	163	29.37	244	2.59	155	31.28
9	212	11.01	149	38.47	254	3.41	154	40.12
RCT – Range Convergence Time								
CCT–Course Convergence Time								
SCT – Speed Convergence Time								

3.2. MoN of MGBEKF

MGBEKF is a stabilized form of EKF i.e., the gain in EKF is modified to attain stability in the estimation process. MoN values with MGBEKF for all scenarios are shown in Figure 5 and the maximum MoN value increasing withan increase in the target course. The maximum MoN values for MGBEKF, to obtain a solution, were observed to be less than 60. The same can be seen from the graph plotted in Figure 5. It can be observed from Table 4 that solution convergence is obtained for target parameters after the MoN reached its maximum value.

3.3. MoN of UKF

For the UKF algorithm, the solution was obtained for the scenarios with maximum MoN values less than 0.01 and greater than 1.9E-04. If the maximum MoN value is greater than 0.01, then the algorithm does not give a consistent solution. UKF uses Unscented transform to reduce the nonlinearity in the process. For this reason, the MoN values are very low as compared to other filtering algorithms. For

Figure 5. MoN values of MGBEKF

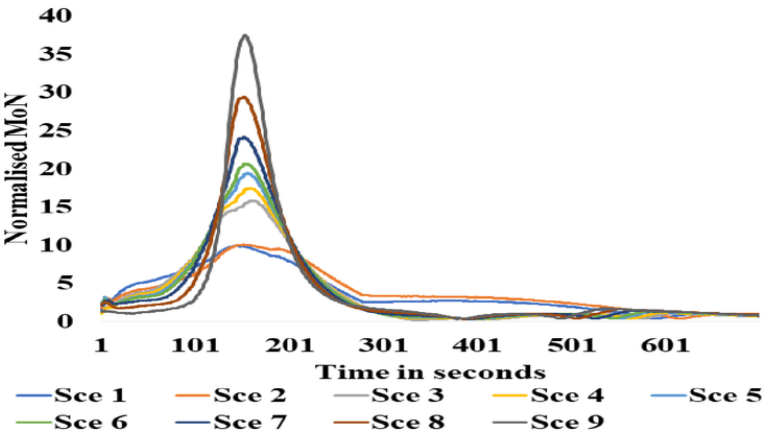

Table 4. Normalized MoN values of MGBEKF at different time samples

Scenario number	RCT	MoN	CCT	MoN	SCT	MoN	Time	Maximum MoN
1	259	3.79	270	3.09	279	2.56	145	9.89
2	257	4.97	265	4.41	281	3.42	153	10.1
3	216	8.09	204	9.95	249	4.21	162	15.9
4	207	9.65	195	12.05	244	4.53	160	17.5
5	201	10.96	188	13.83	232	5.77	157	19.4
6	197	12.03	185	14.99	226	6.51	155	20.7
7	190	14.57	169	21.17	216	8.11	154	24.1
8	184	17.94	156	29.31	203	10.67	154	29.4
9	172	28.04	144	32.23	194	13.43	155	37.4
RCT –Range Convergence Time								
CCT–Course Convergence Time								
SCT–Speed Convergence Time								

the scenarios represented in this paper, the MoN values are as showed in Figure 6. Unlike EKF and MEBEKF, the solution for UKF is obtained before the MoN reaches its maximum value (Table 5).

3.4. Discussion

From the above graphs and data, it can be observed that the solution convergence is obtained after the maximum MoN is reached for EKF and MGBEKF. With EKF, the maximum MoN values has to be greater than 23 to obtain a solution within the acceptance criteria for BOT using observer maneuver recommendation. Similarly, with MGBEKF, the maximum MoN values are supposed to be less than 60 for solution convergence. The nonlinearity in the process is high for the scenarios evaluated using EKF than MGBEKF as MGBEKF is stabilised version of EKF. With UKF, the nonlinearity values are too low as the algorithm completely transforms the nonlinear function to a probability distribution of

Figure 6. MoN values of UKF

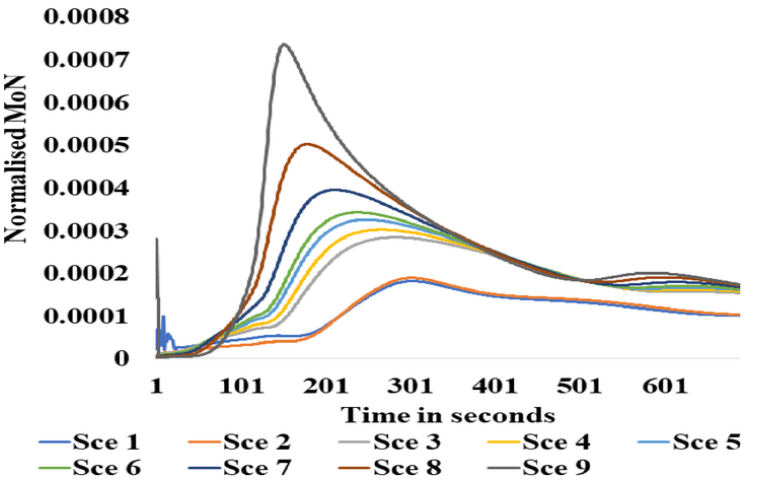

Table 5. Normalized MoN values of UKF at different time samples

Scenario number	RCT	MoN	CCT	MoN	SCT	MoN	Time	Maximum MoN
1	NC	-	738	1.00E-04	NC	-	309	1.82E-04
2	253	1.37E-04	252	1.36E-04	278	1.69E-04	309	1.9E-04
3	216	2.23E-04	199	1.85E-04	249	2.68E-04	304	2.84E-04
4	212	2.51E-04	190	1.98E-04	246	2.93E-04	274	3.03E-04
5	203	2.75E-04	186	2.30E-04	238	3.20E-04	254	3.26E-04
6	200	2.99E-04	183	2.37E-04	231	3.38E-04	256	3.43E-04
7	192	3.68E-04	169	2.89E-04	217	3.94E-04	218	3.95E-04
8	188	5.02E-04	157	3.91E-04	211	4.88E-04	194	5.02E-04
9	198	6.13E-04	146	5.54E-04	223	5.29E-04	164	7.36E-04
RCT–Range Convergence Time								
CCT–Course Convergence Time								
SCT–Speed Convergence Time								

a finite set of statistics whose mean, and covariance is equal to that of the nonlinear function. UKF gives optimized results for BOT with MoN between 1.9E-04 and 0.01.

4. CONCLUSION

An attempt is made to analyze the nonlinearity of the system with respect to different filtering techniques for underwater scenarios using bearings-only measurements. The observations provide limits of nonlinearity for which the filters provide consistent results using bearings-only measurements. With UKF, the nonlinearity in the process is reduced by transforming the function rather than linearizing or using the nonlinearities directly. This helps in obtaining the solution faster and with more accuracy. Observations also show that nonlinearity in the system increases with the target course. It is recommended to use UKF for BOT as it offers low nonlinearity when a few more seconds' extra convergence time is acceptable to the users.

ACKNOWLEDGMENT

This research is supported by the Department of Science and Technology (DST) under the WOS-A scheme via a sponsored project: SR/WOS-A/ET-139/2017(G). The author would like to acknowledge DST and President, Koneru Lakshmaiah Education Foundation (Deemed to be University) for their continuous support and encouragement.

REFERENCES

Aidala, V. J. (1979). Kalman filter behavior in bearings-only tracking applications. *IEEE Transactions on Aerospace and Electronic Systems*, *15*(1), 29–39. doi:10.1109/TAES.1979.308793

Bates, D. M., & Watts, D. G. (1980). Relative curvature measures of nonlinearity. *Journal of the Royal Statistical Society. Series B. Methodological*, *42*(1), 1–25. doi:10.1111/j.2517-6161.1980.tb01094.x

Beale, E. M. L. (1960). Confidence regions in non-linear estimation. *Journal of the Royal Statistical Society. Series B. Methodological*, *22*(1), 41–88. doi:10.1111/j.2517-6161.1960.tb00353.x

Bucci, O. M., Cardace, N., Crocco, L., & Isernia, T. (2001). Degree of nonlinearity and a new solution procedure in scalar two-dimensional inverse scattering problems. *Journal of the Optical Society of America. A, Optics, Image Science, and Vision*, *18*(8), 1832–1843. doi:10.1364/JOSAA.18.001832 PMID:11488487

Dunik, J., Straka, O., Mallick, M., & Blasch, E. (2016). Survey of nonlinearity and non-Gaussianity measures for state estimation. *Proceedings 19th International Conference on Information Fusion*, 1390–1397.

Emancipator, K., & Kroll, M. H. (1993). A Quantitative Measure of Nonlinearity. *Clinical Chemistry*, *39*(5), 766–772. doi:10.1093/clinchem/39.5.766 PMID:8485866

Jones, E., Scalzo, M., Bubalo, A., Alford, M., & Arthur, B. (2011). Measures of nonlinearity for single target tracking problems. *Proceedings of SPIE Signal Processing, Sensor Fusion, and Target Recognition XX*, 8050. doi:10.1117/12.884773

Karthikeyan, T., Sekaran, K., & Ranjith, D. (2019). Personalized Content Extraction and Text Classification Using Effective Web Scraping Techniques. *International Journal of Web Portals*, *11*(2), 41–52. doi:10.4018/IJWP.2019070103

Koteswara Rao, S. (2005). Modified gain extended Kalman filter with application to bearings-only passive manoeuvring target tracking. *IEE Proceedings. Radar, Sonar and Navigation*, *152*(4), 239–244. doi:10.1049/ip-rsn:20045074

Koteswara Rao, S. (2018). Bearings-Only Tracking: Observer Maneuver Recommendation. *Journal of the Institution of Electronics and Telecommunication Engineers*, 1–12. Advance online publication. doi:10.1080/03772063.2018.1535917

Li, X. R. (2012). Measure of Nonlinearity for Stochastic Systems. *Proceedings 15th International Conference on Information Fusion*, 1073–1080.

Liu, Y., & Li, X. R. (2015). Measure of Nonlinearity for Estimation. *IEEE Transactions on Signal Processing*, *63*(9), 2377–2388. doi:10.1109/TSP.2015.2405495

Panigrahi, A., & Bhuyan, K. C. (2017). Fuzzy Logic Based Maximum Power Point Tracking Algorithm for Photovoltaic Power Generation System. *Journal of Green Engineering*, *6*(4), 403–426.

Paul, A., & Raja, S. (2017). An analysis of sampling based techniques in bearing-only tracking. *International Conference on Intelligent Computing, Instrumentation and Control Technologies (ICICICT)*. doi:10.1109/ICICICT1.2017.8342725

Praveen Sundar, P. V., Ranjith, D., & Vinoth Kumar, V. (2020). Low power area efficient adaptive FIR filter for hearing aids using distributed arithmetic architecture. *International Journal of Speech Technology*, *23*(2), 287–296. Advance online publication. doi:10.1007/s10772-020-09686-y

Simon, D. (2006). *Optimal State Estimation: Kalman, H¥ and nonlinear Approximations*. Wiley. doi:10.1002/0470045345

Sultana, H. P., Shrivastava, N., Dominic, D. D., Nalini, N., & Balajee, J.M. (2019). Comparison of Machine Learning Algorithms to Build Optimized Network Intrusion Detection System. *Journal of Computational and Theoretical Nanoscience, 16*(5-6), 2541-2549.

Umamaheswaran, S., Lakshmanan, R., & Vinothkumar, V. (2019). New and robust composite micro structure descriptor (CMSD) for CBIR. *International Journal of Speech Technology*. Advance online publication. doi:10.1007/s10772-019-09663-0

Velliangiri, S., Karthikeyan, P., & Vinoth Kumar, V. (2020). Detection of distributed denial of service attack in cloud computing using the optimization-based deep networks. *Journal of Experimental & Theoretical Artificial Intelligence*, 1–20. Advance online publication. doi:10.1080/0952813X.2020.1744196

Vinoth Kumar, V., Arvind, K. S., Umamaheswaran, S., & Suganya, K. S. (2019). Hierarchal Trust Certificate Distribution using Distributed CA in MANET. *International Journal of Innovative Technology and Exploring Engineering*, *8*(10), 2521–2524. doi:10.35940/ijitee.J9560.0881019

Vinoth Kumar, V., Karthikeyan, T., Praveen Sundar, P. V., Magesh, G., & Balajee, J. M. (2020). A Quantum Approach in LiFi Security using Quantum Key Distribution. *International Journal of Advanced Science and Technology*, *29*(6s), 2345–2354.

Zhang, H., de Saporta, B., Dufour, F., Laneuville, D., & Nègre, A. (2017). Stochastic control of observer trajectories in passive tracking with acoustic signal propagation optimisation. *IET Radar, Sonar & Navigation*, *12*(1), 112–120. doi:10.1049/iet-rsn.2017.0123

Zhu, , Xu, , Li, , & Wu, . (2012). Research on the Observability of Bearings-only Target Tracking Based on Multiple Sonar Sensors. *Second International Conference on Instrumentation, Measurement, Computer, Communication and Control*, 631 – 634. doi:10.1109/IMCCC.2012.154

Kausar Jahan, research scholar in Koneru Lakshmaiah Educational Foundation, Vaddeswaram, Guntur, AP, India. She completed her B. Tech in 2009 at JNTU Kakinada and M Tech in 2015 at JNTU Kakinada in ECE. She is presently working as women scientist WOS-A.

S. Koteswara Rao, former scientist "G" in NSTL, DRDO, Visakhapatnam is currently working as Professor in Koneru Lakshmaiah Education Foundation, Vaddeswaram, Guntur, AP, India. He received BTech in 1977 at JNTU and ME in 1979, PSG college of technology, Coimbatore and Ph. D at Andhra University all in Electrical Engineering. He published several papers in International Conference & Journals in the field of signal processing. He is the fellow member of IETE.